X-Ray Generation by the Smith-Purcell Effect

Michael J. Moran

Lawrence Livermore National Laboratory, University of California, L-41, P.O. Box 808, Livermore, California 94550

(Received 12 June 1992)

Smith-Purcell (S-P) radiation is produced when electrons graze the surface of a grating. Calculations based on the theory of diffraction radiation show that, given severe restrictions on e^--beam quality, S-P radiation is highly efficient. Efficient S-P x-ray generation requires relativistic e^- beams having a transverse momentum and dimension whose product approaches the Heisenberg uncertainty limit.

PACS numbers: 41.60.−m, 07.85.+n

The Smith-Purcell (S-P) effect is the production of radiation by electromagnetic interaction between electrons in motion and grooves in the surface of a grating [1,2]. The S-P effect produces coherent, narrow-band radiation from the radio to ultraviolet spectral regions with electrons having kinetic energies of 50 keV or more. These characteristics have evoked ideas for novel devices and applications such as the Varatron for voice communications [3], or the Orotron, a tunable mm-wave oscillator [4]. Further work has considered adapting these devices for use as free-electron lasers (FEL) [5–8].

Advances in e^--beam and x-ray technologies have led to studies of S-P x-ray production [8–11], and even to some rather optimistic speculation on the possibility of an S-P x-ray FEL [12]. However, contrary to experience with longer wavelengths [1,3–5,13], S-P radiation having wavelengths shorter than, say, 1000 Å has yet to be observed.

The purpose here is to present a combination of theoretical results that will support the design of careful S-P x-ray experiments. Here, the S-P effect refers to an interaction between a freely propagating electron and a gratinglike structure. This should not be confused with S-P FELs, where the main interaction is between the electron and the space harmonics of a photon field (S-P is attached to the name of such FELs because a diffraction grating assists in establishing the photon field) [14].

This paper uses a new calculational approach to study some specific aspects of S-P x rays in the spontaneous-emission, single-particle limit: emission distributions in forward directions for gratings with a finite number of grooves. X rays probably will be easiest to observe in the forward direction, where S-P wavelengths will be shortest. The results show that S-P x-ray generation is a tightly constrained process in which the finite lengths of gratings must be considered. S-P x-ray production requires that the e^- beam be steered extremely close to the grating (within hundreds of Å) without striking its surface. If electrons strike the surface, then the S-P radiation may be overwhelmed by transition radiation (TR) or other mechanisms.

The present calculations use an *ad hoc* theoretical description which is adapted from one simple case in the theory of diffraction radiation [15], that of a single electron that radiates as it passes through a single linear slit (see Fig. 1). The electron has relativistic speed $\beta=v/c$ in the z direction, where v is the electron speed and c the speed of light. The slit, with width w_s, is in an infinite opaque screen (of zero thickness in the x-y plane at $z=0$).

Ter-Mikaelian [16] has obtained a closed-form solution for the radiation produced by this interaction:

$$\frac{d^2N}{d\omega\, d\Omega}=2\pi^2\left(\frac{\omega}{\hbar c}\right)(|E_x|^2+|E_y|^2)\,, \tag{1}$$

$$E_x=i\kappa\left(\frac{k_x}{f}\right)\left(\frac{e^{-y_-(f-ik_y)}}{f-ik_y}+\frac{e^{-y_+(f+ik_y)}}{f+ik_y}\right),$$

$$E_y=\kappa\left(\frac{e^{-y_-(f-ik_y)}}{f-ik_y}-\frac{e^{-y_+(f+ik_y)}}{f+ik_y}\right),$$

where dN is the number of photons with radial frequency ω that are radiated into bandwidth $d\omega$ and solid angle $d\Omega$. E_x and E_y are the x- and y-polarized electric field amplitudes, respectively. Also, $e=4.8\times10^{-10}$ esu, $c=3\times10^{10}$ cm/sec, $\hbar=1.05\times10^{-27}$ ergsec, $\kappa=e/4\pi^2c$, $k=\omega/c$, $k_x=k\sin\theta\cos\phi$, $k_y=k\sin\theta\sin\phi$, $f=(k_x^2+\eta^2)^{1/2}$, and $\eta=\omega/\gamma v$. Here, θ and ϕ are the polar angles for the direction of emission. Finally, y_+ and y_- are the distances of the electron from the top and bottom of the slit, respectively ($y_++y_-=w_s$; see Fig. 1). The field amplitudes in Eq. (1) combine to give the total field $\mathbf{E}_1$ radiated by the slit:

$$\mathbf{E}_1=E_x\hat{\mathbf{x}}+E_y\hat{\mathbf{y}}\,. \tag{2}$$

This result can be used to model radiation produced by a series of such slits. For example, if the slit in Fig. 1 is

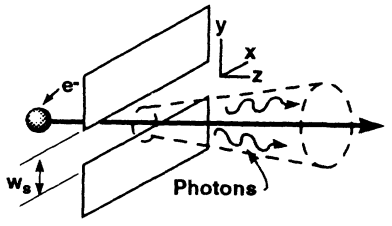

FIG. 1. Single-slit diffraction-radiation geometry.

© 1992 The American Physical Society

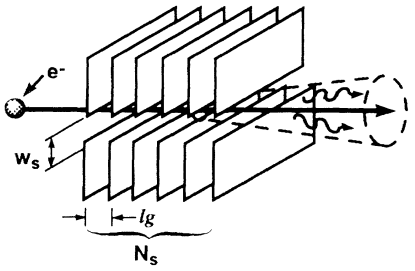

FIG. 2. Radiation generation in a periodic-slit array.

followed at a distance l_g by an identical second slit, then the radiation generated by interaction with the second slit $\mathbf{E}_2$ is

$$\mathbf{E}_2 = e^{i\Phi}\mathbf{E}_1 , \tag{3}$$

where Φ describes the "retarded" phase delay associated with radiation generated at the second slit:

$$\Phi = 2\pi(l_g/\lambda\beta)(1-\beta\cos\theta) , \tag{4}$$

with $\lambda = 2\pi/k$. Equation (3) is accurate only to the extent that the electron is unaffected by its interaction with the first slit. Here, this requires that the energy radiated at the first slit be a small fraction of the electron kinetic energy. The present case uses photon energies below 1 keV, and electron kinetic energies above 1 MeV. Repetition of this process describes the radiation generated by N_s equally spaced slits, as illustrated in Fig. 2, to give the total radiated field:

$$\mathbf{E}_{\rm tot} = \sum_{n=1}^{N_s} e^{i(n-1)\Phi}\mathbf{E}_1 . \tag{5}$$

This result can be used to model the S-P effect by using a very large slit width ($w_s \gtrsim 1$ cm) and having the electron pass very close to the slits' bottom edges ($y_- \ll w_s$). For this case, the formulas above describe basic emission characteristics of S-P radiation, such as angular and spectral intensity distributions, and their dependences on the number of "grating" grooves, the electron kinetic energy, the photon energy, the grazing "impact parameter," y_-, etc.

While Eqs. (1)–(5) provide a description of the basic characteristics of S-P radiation, there are also a number of issues that cannot be addressed. For example, since the "ridges" of the grating surface are modeled by the edges of ideal slits, this approach cannot model blazed gratings. However, the results should be appropriate for radiation generated by so-called laminar gratings (i.e., with a square-wave groove profile) having periods much greater than the widths of the individual ridges. Also, aspects such as actual complex dielectric constants for different materials, surface quality, unaccounted electromagnetic modes of the grating structure, or energy absorption by the grating structure will require detailed studies for the specific cases of interest.

In spite of these limitations, the present model is useful for its descriptions of various basic characteristics of S-P emission. The model describes emission distributions for any angle and frequency of interest, but the discussion will be devoted mostly to forward angles of emission (i.e., $\theta \ll 1$). This is because constructive interference and the relativistic contraction that is implicit in Eq. (4) will emphasize shorter wavelengths in forward directions [see discussion of Eq. (6) below].

Figure 3 shows a specific case of forward-directed angular distributions of "x"- and "y"-polarized 100-eV S-P photons. The total integrated photon yield for this case is about 5×10^{-6} photon/electron eV. The radiation, which is more than 98% "y" polarized, has a y-polarized part that is a round, narrow, forward-directed beam, with an on-axis maximum and an angular FWHM of about 20 mrad. The "x" polarization, with an on-axis zero, has a very different angular distribution.

The "x" and "y" intensity distributions are sensitive to the system parameters. Figure 3 shows the case of a wide slit with $2\pi y_-/\gamma\beta\lambda \approx 0.5$. When the slit is "narrow" (i.e., $2\pi w_s/\gamma\beta\lambda \leq 0.1$), then the "$x$" and "$y$" intensities are similar. When electrons pass through the center of a

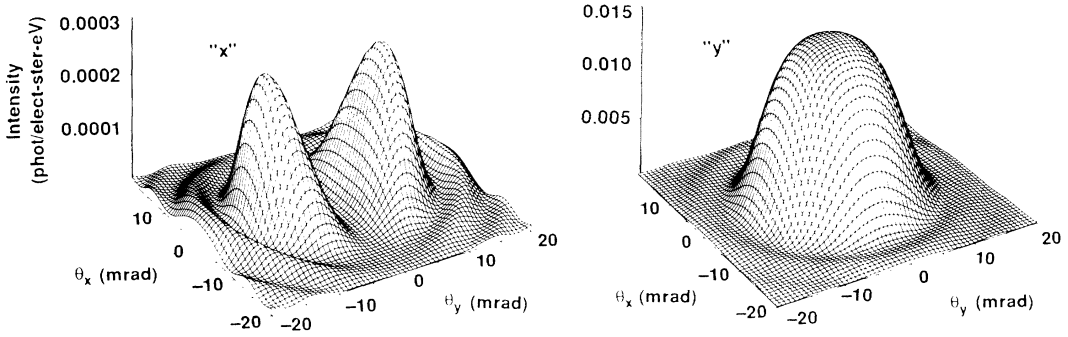

FIG. 3. "x"- and "y"-polarized emission distribution for 100-eV photons radiated by 10-MeV electrons passing 200 Å away from the bottom slits of a ten element array having a slit width of 1 cm and a period of 10.5 μm. Here, $\theta_x = \theta\cos\phi$ and $\theta_y = \theta\sin\phi$.

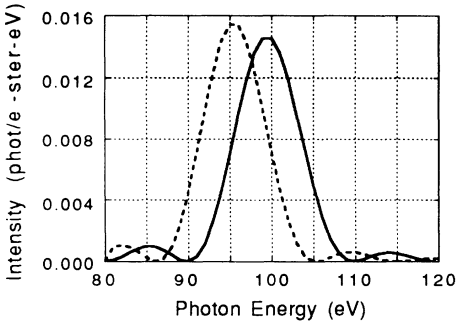

FIG. 4. Smith-Purcell emission spectra.

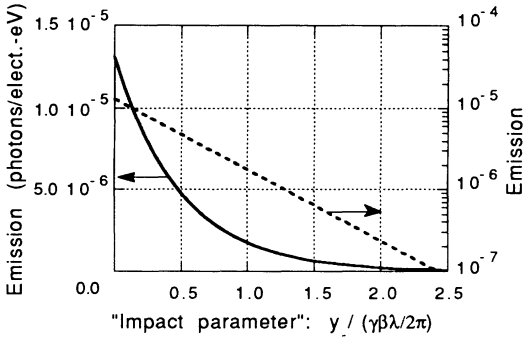

FIG. 5. Intensity vs "impact parameter."

narrow slit, the "x" and "y" intensities are the same, with on-axis minima and maxima in the x-z and y-z planes, respectively. The total intensity distribution in this case takes the form of a TR-like cone (having an on-axis zero and polarization in the plane of emission), with intensities that are virtually the same as for corresponding TR multiple-foil radiators [17]. This is as it should be: In the limit that $2\pi w_s/\gamma\beta\lambda \rightarrow 0$, the slits become continuous foils, as in TR.

The photon energy spectrum is determined by a combination of the basic spectrum from a single slit [described by Eq. (1)] and interference between contributions from successive slits in the array. Those wavelengths λ_r that interfere constructively can be obtained by setting $\Phi = 2\pi r$, where r is any positive integer, in the Doppler shift formula [Eq. (4)]. In forward directions ($\theta \ll 1$), for $\gamma \gg 1$, and for the lowest-order mode ($r = 1$), this gives the familiar relativistic-contraction formula:

$$\lambda_r \approx (l/2\gamma^2)(1+\gamma^2\theta^2)\,. \tag{6}$$

Higher-order modes ($r > 1$) will not be discussed, because, in the x-ray spectral region, they usually will be present with intensities much smaller than those for $r = 1$.

Figure 4 shows spectra calculated for the device described above, with on-axis and $\theta = 10$ mrad angles of emission in the x-z plane. The on-axis spectrum (solid line) is centered near 100 eV, with roughly a 10% bandwidth. One hundred eV is consistent with relativistic contraction of the 10.5-μm period of the slit array [see Eq. (6)], and the 10% bandwidth is indicative of constructive interference of contributions from each of the ten slits. The 10-mrad spectrum (dashed line) is similar, but with the center energy reduced to about 96 eV, consistent with Eq. (6).

The S-P photon emission depends on N_s in an intuitive fashion. Increasing N_s increases the photon yield in proportion to N_s, while the on-axis spectral intensity increases with N_s^2. The corresponding energy spectrum narrows in proportion to $1/N_s$, while the angular distribution narrows with $1/N_s^{1/2}$.

The calculations also can be used to study the dependence of radiated intensity on the "impact parameter," y_-. Using the same conditions as for Fig. 3, Fig. 5 shows linear and semilog plots of the on-axis 100-eV emission intensity versus y_-, in units of $\gamma\beta\lambda/2\pi$. The linear plot illustrates a "useful" range for y_-: The radiated intensity is relatively small for $y_- > \gamma\beta\lambda/2\pi$, but little is gained as y_- decreases below $y_- \approx 0.1\gamma\beta\lambda/2\pi$. The semilog plot, a straight line, indicates that the intensity declines exponentially to very small values as y_- increases beyond $\gamma\beta\lambda/2\pi$ [6,7,18,19]. Thus, we have the requirement

$$y_- < \gamma\beta\lambda/4\pi\,, \tag{7}$$

if efficient emission is desired.

The results in Fig. 5 are interesting in a more general sense. The "ultimate" emission efficiency of about 1.3×10^{-5} photon/electron eV (per 10 slits) approaches the limit for coherent interaction with an isolated electron [20]. Whether for TR, synchrotron radiation, or some other similar mechanism, the maximum efficiency N_{phot} that can be expected from a single interaction is approximately [10,20]

$$N_{\text{phot}} \approx (2\alpha/\pi)(d\omega/\omega)\ln(A\gamma)\,, \tag{8}$$

where $\alpha = \frac{1}{137}$ and A is a constant that depends on the radiation mechanism. N_{phot} is the spectral density of a relativistic electron's Coulomb field [21]. In effect, N_{phot} is the spectral density that is available to be radiated in a given interaction. Thus, S-P radiation can be highly efficient—both in absolute terms, and relative to other efficient radiation mechanisms.

The discussion above can be pursued further to study S-P x-ray generation by electron beams having finite sizes. The basic constraint in Eq. (7) is that, if an electron does not pass close enough to the surface to excite the desired frequencies, then those frequencies will not be radiated. For beams with finite diameters, the total radiated field is just the superposition of fields due to the individual electrons. Thus, only that portion of the beam satisfying Eq. (7) will radiate by the mechanism described above.

Figure 6 illustrates an appropriate geometry for studying this issue. Equation (7) leads to two simultaneous requirements. First, in order for the *entire* beam to interact

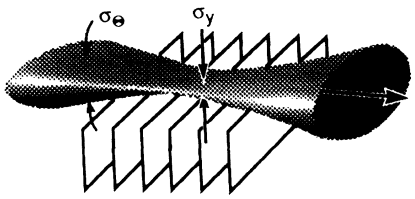

FIG. 6. Smith-Purcell beam geometry.

strongly, it must have a size $\sigma_y < \gamma\beta\lambda/4\pi$. At the same time, in order for the beam to interact efficiently over the entire length of the grating, without striking the surface, the beam must have angular divergence $\sigma_\theta < (\gamma\beta\lambda/4\pi)/N_s^* l_g$. Combining these two constraints defines the emittance ε_y that the electron beam must achieve:

$$\varepsilon_y \leq \sigma_y \sigma_\theta \approx \lambda/32\pi^2 N_s . \quad (9)$$

A beam with this emittance could be "steered" to interact effectively over the entire length of the grating. Surprisingly, Eq. (9) indicates that the required emittance depends on the desired wavelength and the number of elements in the grating, but not on the electron energy. Thus, although higher electron energies allow larger impact parameters [Eq. (7)], higher energies also lead to greater grating periods [see Eq. (6)] and longer overall structures.

While the requirement in Eq. (9) is extremely severe, it may be possible to achieve for some specific situations. For photons in the 100-eV to 1-keV spectral range, and for electron energies of tens of MeV, Eq. (9) amounts to requiring that e^- beams have a transverse momentum Δp_y and a width Δy whose product approaches the Heisenberg uncertainty limit ($\Delta y \Delta p_y \geq \hbar$). To see this, recall that $\Delta p_y \approx \gamma m_e c \sigma_\theta$, so that $\Delta y \Delta p_y \approx \gamma m_e c \sigma_\theta \sigma_y$. For the conditions in Fig. 3, we obtain $\Delta y \Delta p_y \approx 2.3 \times 10^{-25}$ erg sec, somewhat greater than $\hbar$. However, attempts to increase the photon emission efficiency or to reduce the spectral bandwidth by increasing N_s can lead quickly to beam-quality requirements that violate the uncertainty principle.

Finally, note that although the radiated power may be low, the source *brightness* could be surprisingly large, because of the microscopic source area. This, together with the tunability and inherent spatial coherence of S-P radiation, suggests possible applications in the area of x-ray microscopy or microholography.

The author thanks James Morgan for reviewing the manuscript and Britton Chang for guidance on some mathematical issues. This work was performed under the auspices of the U.S. Department of Energy by the Lawrence Livermore National Laboratory under Contract No. W-7405-ENG-48.

[1] S. J. Smith and E. M. Purcell, Phys. Rev. **92**, 1069 (1953).
[2] While the name derives from the authors of Ref. [1], work by W. Salisbury on this topic led to a somewhat earlier patent award. See U.S. Patent No. 2634372 (1953).
[3] See Electronics **74**, Oct. 19 (1962).
[4] F. S. Rusin and G. D. Bogomolov, Proc. IEEE **57**, 720 (1969).
[5] E. M. Marshall *et al.*, IEEE Trans. Plasma Sci. **16**, 199 (1988).
[6] A. Gover and P. Sprangle, IEEE J. Quantum Electron. **17**, 1196 (1981).
[7] R. P. Leavitt *et al.*, IEEE J. Quantum Electron. **17**, 1333 (1981).
[8] J. M. Wachtel, J. Appl. Phys. **50**, 49 (1979).
[9] G. Doucas *et al.*, Bull. Am. Phys. Soc. **37**, 934 (1992).
[10] M. J. Moran and B. Chang, in *Proceedings of the Twelfth Werner Brandt International Conference on the Penetration of Charged Particles in Matter, San Sebastian, Spain* (National Technical Information Service of the U.S. Department of Commerce, 1989), CONF-8909210, p. 537.
[11] J. Walsh (private communication).
[12] D. B. Chang and J. C. McDaniel, Phys. Rev. Lett. **63**, 1066 (1989).
[13] D. E. Wortman *et al.*, IEEE J. Quantum Electron. **17**, 1341 (1981).
[14] J. Walsh, IEEE J. Quantum Electron. **21**, 920 (1985).
[15] B. M. Bolotovskii and G. V. Voskresenskii, Usp. Fiz. Nauk. **88**, 209 (1966); **94**, 377 (1968) [Sov. Phys. Usp. **9**, 73 (1966); **11**, 143 (1968)].
[16] M. L. Ter-Mikaelian, *High-Energy Electromagnetic Processes in Condensed Media* (Wiley-Interscience, New York, 1972), p. 382.
[17] M. A. Piestrup *et al.*, Phys. Rev. A **32**, 917 (1985).
[18] J. P. Bacheimer, Phys. Rev. B **6**, 2985 (1972).
[19] C. W. Barnes and K. G. Dedrick, J. Appl. Phys. **37**, 411 (1966).
[20] P. L. Csonka, Phys. Rev. A **35**, 2196 (1987).
[21] W. K. Panofsky and M. Phillips, *Classical Electricity and Magnetism* (Addison-Wesley, Cambridge, MA, 1955), p. 382.

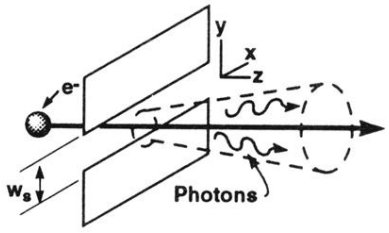

FIG. 1. Single-slit diffraction-radiation geometry.

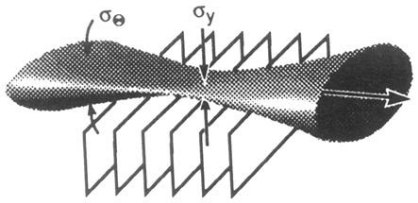

FIG. 6. Smith-Purcell beam geometry.